A New Family of Bismuth-Based Oxide Materials: $Bi_{2-2x}U_xLa_xO_{(3+3x/2)}$ ($0.333 \geq x \geq 0.038$): Synthesis, Characterization, and Phase Transformations on Aging

J. M. Amarilla and R. M. Rojas*

Instituto de Ciencia de Materiales de Madrid, Consejo Superior de Investigaciones Científicas, Serrano 113, 28006 Madrid, Spain

Received July 25, 1995. Revised Manuscript Received October 18, 1995[⊗]

A series of Bi_2O_3-based oxides of general formula $Bi_{2-2x}U_xLa_xO_{(3+3x/2)}$ ($0.333 \geq x \geq 0.038$) has been synthesized by two different methods. Materials were characterized by X-ray diffraction, chemical analysis, X-ray photoelectron spectroscopy, and thermal analysis. X-ray diffraction data show that they crystallize with cubic or hexagonal symmetry depending on composition and synthesis procedure. In particular, the stabilization of the fluorite-type structure as a single phase at room temperature has been achieved in the compositional range $0.154 \geq x \geq 0.091$. The annealing of materials at 600 °C for 500 h yields in all cases a "tetragonal" phase that is isolated as the only phase for $x = 0.222$. The evolution of this phase with temperature has been studied. Aged materials can be regenerated when they are subjected to the original synthesis conditions.

Introduction

Compounds that exhibit predominantly oxygen ion conduction are found mainly among solid solutions based of oxides of tetravalent metals doped with lower valent metals, crystallizing with the fluorite-type structure.[1] Among them, yttria- or calcia-stabilized zirconias constitute typical examples. They have found many applications, mainly as electrolytes in solid oxide fuel cells (SOFCs) and in oxygen sensors.[2,3] However, the range of application is limited by the too low oxide-ion conductivity below 800 °C. Consequently, searching of new oxygen ion conductors with high conductivity at lower temperatures is of interest. It is well-known that Bi_2O_3 exhibits a remarkable range of useful solid-state properties. The high-temperature form, δ-Bi_2O_3, is one of the best ionic conductors.[4] The crystal structure of this phase belongs to the defect fluorite-type structure, with 25% vacant sites in the anionic sublattice. Solid solutions derived from Bi_2O_3 doped with a great number of aliovalent cations ranging from 2^+ to 6^+ constitute a series of materials that are characterized by their high oxide ion conductivity at low temperatures,[5−7] the values of which are at least an order of magnitude greater than that of, i.e., yttria-stabilized zirconia.[2] With regard to possible applications, the thermal and chemical stabilities of stabilized δ-Bi_2O_3 are of great interest. However, it has been discussed whether the high-temperature δ-Bi_2O_3 is really stabilized by an oxide additive, or the reported face-centered cubic phases are metastable phases obtained in the bismuth-rich region of each system.[8] Therefore, δ-phases destabilize on annealing and gradually transform into the stable low-temperature modification[9] or decompose into a mixture of phases.[8] Representative examples are the $R\bar{3}m$ layered structures formed in the Bi_2O_3−Ln_2O_3 (Ln = lanthanide, Y, Pr, Er), isomorphous with those described for some mixed alkaline earth−bismuth oxides[10] or the tetragonal $I4_1/a$ β-Bi_2O_3-like phases described in the Bi_2O_3−WO_3[11,12] system. In some cases, destabilization can be suppressed by the addition of aliovalent dopants such as ZrO_2, to avoid cation interdiffusion.[13]

To date, the Bi_2O_3-based systems reported in the literature are mostly binary oxides. However, it has been indicated that Bi_2O_3-based oxides containing two dopants have higher conductivity, and systems with double oxides dopant have been described.[14] Moreover, it has been recently shown that the stabilization of the fluorite-type phase can also be achieved when Bi^{3+} ion is simultaneously substituted for a divalent and a pentavalent ion in 1/1 ratio.[15] According to this, we have considered worthwhile to investigate the oxides formed when Bi_2O_3 is simultaneously doped with U/La in molar ratio 1:1. In the present work the synthesis and characterization of a new series of Bi_2O_3-based mixed oxides of general formula $Bi_{2-2x}U_xLa_xO_{(3+3x/2)}$ in the compositional range $0.333 \geq x \geq 0.038$ is reported.

[⊗] Abstract published in *Advance ACS Abstracts*, December 1, 1995.

(1) Dell, R. M.; Hooper, A. In *Solid Electrolytes*; Hagenmuller, P., van Gool, W., Eds.; Academic Press: San Diego, 1978; p 291.
(2) Etsell, T. H.; Flengas, S. N. *Chem. Rev.* **1970**, *70*, 339.
(3) Steele, B. C. H. In *Electronic Ceramic*; Steele, B. C. H., Ed.; Elsevier: London, 1991; p 203.
(4) Takahashi, T.; Iwahara, H. *Mater. Res. Bull.* **1978**, *13*, 1447.
(5) Burggraaf, A. J.; Boukamp, B. A.; Vinke, I. C.; de Vries, K. J. In *Advances in Solid-State Chemistry*; Catlow, C. R. A., Ed.; Jai Press: London, 1989; Vol. 1, p 259.
(6) Takahashi, T. In *Superionic Solids and Solids Electrolytes. Recent Trends*; Laskar, A. L., Chandra, S., Eds.; Academic Press Inc.: San Diego, 1989; p 1.
(7) Azad, A. M.; Larose, S.; Akbar, S. A. *J. Mater. Sci.* **1994**, *29*, 4135.
(8) Watanabe, A. *Solid State Ionics* **1990**, *40/41*, 889.
(9) Jiang, N.; Buchanam, R. M.; Stevenson, D. A.; Nix, W. D.; Li, J.-Z.; Yang, J.-L. *Mater. Lett.* **1995**, *22*, 215.
(10) Conflant, P.; Boivin, J. C.; Thomas, D. *J. Solid State Chem.* **1980**, *35*, 1992.
(11) Watanabe, A.; Ishizawa, N.; Kato, M. *J. Solid State Chem.* **1985**, *60*, 252.
(12) Zhou, W. *J. Solid State Chem.* **1994**, *108*, 381.
(13) Fung, K. Zong; Baek, H. D.; Vikar, A. V. *Solid State Ionics* **1992**, *52*, 199.
(14) Meng, G.; Chen, Ch.; Han, X.; Yang, P.; Peng, D. *Solid State Ionics* **1988**, *28−30*, 533.
(15) Laroussi, B. F.; Khairoun, S.; Tressaud, A.; Réau, J. M. *J. Alloys Compd.* **1993**, *200*, 19.

0897-4756/96/2808-0401$12.00/0

Materials were characterized by X-ray diffraction, chemical analysis, X-ray photoelectron spectroscopy, and thermal analysis. In particular, the stabilization of the fluorite-type structure as a single phase at room temperature has been achieved in the compositional interval $0.154 \geq x \geq 0.091$. Results obtained show that the materials crystallize with cubic, hexagonal, or "tetragonal" symmetry depending on composition, conditions of synthesis, and/or annealing periods. The structure of the hexagonal phases can be derived from the reported for the high-temperature Bi_2UO_6,[16] while the "tetragonal" phase is closely related to tetragonal β-Bi_2O_3.[17]

Experimental Section

Mixed bismuth uranium lanthanum oxides were prepared by two alternative routes; either by a mixed ceramic/organic precursor procedure or by the traditional ceramic method. The first one is based on the reaction

$$(1-x)Bi_2O_3 + xLaUO_2(C_2H_5COO)_5{\cdot}3H_2O \xrightarrow[950\ ^\circ C\ 24\ h,\ air]{Pt\ crucible} Bi_{2-2x}U_xLa_xO_{(3+3x/2)}$$

Stoichiometric amounts of monoclinic bismuth oxide α-Bi_2O_3 and lanthanum uranyl propionate $LaUO_2(C_2H_5COO)_5{\cdot}3H_2O$, with Bi:U:La ratios ranging from 4:1:1 to 50:1:1 ($0.333 \geq x \geq 0.038$) were intimately mixed by grinding in an agate mortar. The mixtures were heated at 10 °C min^{-1} to 850 °C and then at 1 °C min^{-1} up to 950 °C and kept at this temperature for 24 h (*method I*). Samples obtained by this procedure will be referred hereafter as **S*N***, where ***N*** stands for bismuth in the Bi:U:La = ***N***:1:1 ratio. Batches of each composition were either quenched to room temperature or allowed to cool within the furnace. Batches of the slowly cooled samples were annealed at 600 °C for 50 or 500 h.

To grow single crystals, appropriate amounts of α-Bi_2O_3 and lanthanum uranate $LaUO_{4+x}$ obtained from thermal decomposition at 850 °C of the organic precursor lanthanum uranyl propionate were thoroughly mixed. The mixtures were situated in covered plantinum crucibles, heated at 2 °C min^{-1} to 950 °C and kept at this temperature for 24 h, and then they were cooled at 2 °C h^{-1} to 600 °C and then at 2 °C min^{-1} to room temperature. This method was not successful, but it yielded polycrystalline materials having showed some structural differences with those synthesized by the mixed ceramic/organic precursor method. These samples synthesized by *method II* will be referred as **C*N***; the meaning of ***N*** is identical with that described before. These products were also annealed at 600 °C for 50 or 500 h and then allowed to cool within the furnace.

X-ray powder diffraction patterns were recorded with a Siemens D-501 diffractometer, with Cu Kα radiation. Diagrams were scanned at 0.02° (2θ) and 1 or 5 s/step counting time. The scans have been made in the range $4 \leq 2\theta \leq 80°$, and the unit-cell parameters have been refined using the program CELREF.[18] Uranium and lanthanum content has been determined by inductive coupled plasma (ICP) method with a Perkin-Elmer Plasma 40 emission spectrometer; the content of bismuth has been analyzed with a Pye-Unicam SP9 atomic absorption spectrophotometer. Differential thermal analysis (DTA) and thermogravimetric (TG) curves have been simultaneously recorded on Stanton STA 781 instrument. A ≈80−100 mg sample has been heated at several temperatures at 10 °C min^{-1} heating and heating/cooling rates in still-air atmosphere; α-Al_2O_3 has been used as reference material. X-ray photoelectron (XPS) spectra have been recorded in a VG-ESCALAB 210 photoelectron spectrometer with Mg Kα radiation, in the pass energy mode at 50 eV. Calibration was achieved using C1s peak at 284.6 eV, and samples were examined in the form of pellets.

Characterization of materials synthesized using *methods I* and *II* are reported below; studies carried out for annealed materials are also indicated.

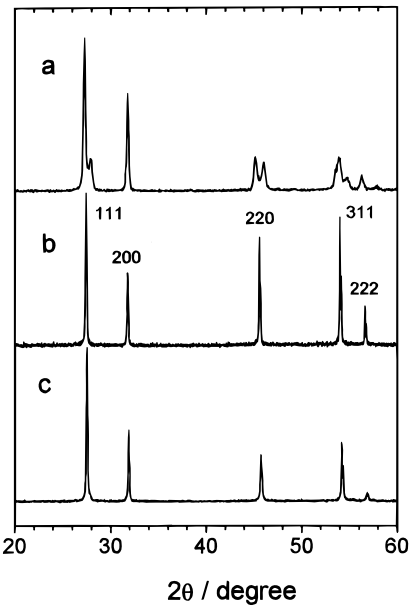

Figure 1. X-ray diffraction patterns of $Bi_{2-2x}U_xLa_xO_{(3+3x/2)}$ synthesized by method I: (a) $x = 0.250$ (**S6**) cooled to room temperature; (b) **S6** quenched from 950 °C (fcc-type phase); (c) $x = 0.133$ (**S13**) cooled to room temperature.

Table 1. Experimental Cell Parameters for Hexagonal $Bi_{2-2x}U_xLa_xO_{3+3x/2}$: Method I, Samples S; Method II, Samples C

	composition		cell parameters (Å)		
sample	Bi:U:La	x^a	a_h	c_h	c_h/a_h
S4	4:1:1	0.333	3.9937(8)	9.728(2)	2.436
C4	4:1:1	0.333	4.027(1)	9.547(2)	2.371
S5	5:1:1	0.286	4.020(1)	9.576(2)	2.382
C5	5:1:1	0.286	4.0262(4)	9.547(1)	2.371
S6	6:1:1	0.250	4.017(2)	9.537(6)	2.374
C6	6:1:1	0.250	4.0168(8)	9.545(2)	2.376
C7	7:1:1	0.222	4.0066(7)	9.543(2)	2.383
C8	8:1:1	0.200	4.0079(7)	9.539(2)	2.380
S9	9:1:1	0.182	3.998(2)	9.550(5)	2.389
S10	10:1:1	0.167	3.992(2)	9.608(5)	2.407
C10	10:1:1	0.167	4.006(2)	9.549(4)	2.384

[a] Mol % dopant = 100x.

Results

X-ray powder diffraction data show that the structural type of the phases obtained depends on the synthesis conditions. Figure 1 shows X-ray powder patterns of some materials synthesized by the mixed ceramic/organic precursor procedure (*method I*). They crystallize with two different structures. Samples with 33.3 (**S4**) to 16.7 (**S10**) mol % dopant cooled to room temperature, show similar X-ray patterns (Figure 1a). They have been indexed on the basis of a hexagonal cell and the lattice parameters are summarized in Table 1. In the same compositional range, quenching of the samples from the synthesis temperature (950 °C) yields face-centered cubic (fcc) materials as the only phases (Figure 1b, Table 2). Nevertheless, it is worth noting that the samples containing 15.4 (**S11**) to 11.8 (**S15**) mol % dopant and cooled to room temperature are fluorite-type

(16) Amarilla, J. M.; Rojas, R. M.; Herrero, P. *Chem. Mater.* **1995**, *7*, 341.
(17) Blower, S. K.; Greaves, C. *Acta Crystallogr.* **1988**, *C44*, 587.
(18) Laugier, J.; Filhol, A. (CELREF), I.L.L. Grenoble, France, unpublished, P.C. version, 1991.

Table 2. Experimental Cell Parametrs for Cubic $Bi_{2-2x}U_xLa_xO_{3+3x/2}$: Method I, Samples S; Method II, Samples C

	composition		cell parameters
sample[a]	Bi:U:La	x[c]	a_c (Å)
C4[a]	4:1:1	0.333	5.641(1)
S4[a]	4:1:1	0.333	5.6378(1)
S5[a]	5:1:1	0.286	5.6339(1)
S6[a]	6:1:1	0.250	5.6331(9)
S9[a]	9:1:1	0.182	5.619(2)
S10[a]	10:1:1	0.167	5.6155(1)
S11	11:1:1	0.154	5.6136(8)
C12.5	12.5:1:1	0.138	5.6079(5)
S13	13:1:1	0.133	5.6061(3)
C15	15:1:1	0.118	5.606(2)
S15	15:1:1	0.118	5.6038(2)
S16	16:1:1	0.111	5.6040(9)
S17	17:1:1	0.105	5.605(1)
C20	20:1:1	0.091	5.597(2)
S25[b]	25:1:1	0.074	5.601(2)
S50[b]	50:1:1	0.038	5.602(1)

[a] Quenched from 950 °C. [b] Mixtures of cubic fluorite and α-Bi_2O_3. [c] Mol % dopant = 100x.

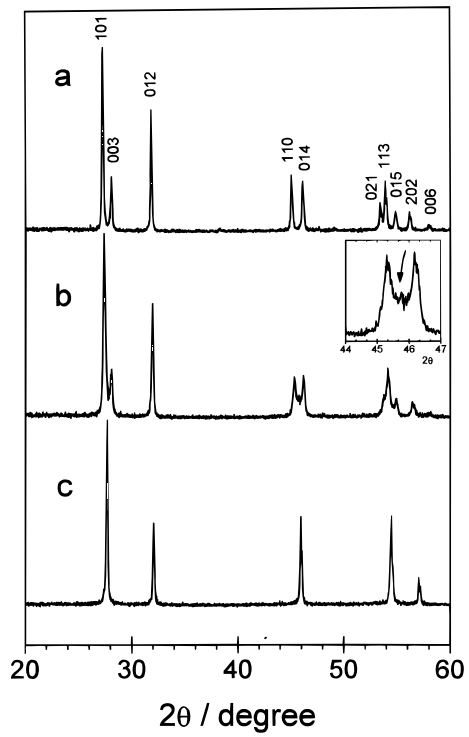

Figure 2. X-ray diffraction patterns of $Bi_{2-2x}U_xLa_xO_{(3+3x/2)}$ synthesized by method II: (a) a = 0.333 (hexagonal **C4**); (b) x = 0.167 (**C10**, the arrowed peak is the reflection (220) of the fcc-type phase); (c) x = 0.091 (**C20**).

single phases (Figure 1c, Table 2). From 11.1 (**S16**) to 3.85 (**S50**) % mol dopant, a mixture of fcc and α-Bi_2O_3 is formed (Table 2). However, for samples **S16** and **S17**, the amount of α-Bi_2O_3 is very low and diffraction maxima of this impurity are hardly observed.

Figure 2 shows X-ray powder diagrams of some materials synthesized by *method II*. Patterns recorded for samples with composition 33.3 (**C4**) to 16.7 (**C10**) mol % have also been indexed on the basis of a hexagonal cell (Figure 2a,b). The cell parameters are summarized in Table 1. A closer inspection of the pattern shown in Figure 2b reveals the presence of additional peaks ascribed to the fcc phase, that is particularly evident in the 44−47° (2θ) range. A magnification of this region is presented in the inset of Figure 2b and the reflection (220) of the fluorite phase is arrowed. This mixture can be identified for samples with 16.7−13.8 mol % dopant. For lower dopant concentration, 11.8 (**C15**) to 9.1 (**C20**) mol % dopant, materials crystallize with the fluorite-type structure. In Figure 2c the diagram of the sample **C20** is presented.

Results from chemical analysis for bismuth, uranium, and lanthanum carried out on materials obtained by both procedures indicate that there is no appreciable deviation from the starting nominal compositions. Mg Kα X-ray photoelectron spectra of the U4f and Bi4f core levels and U5f, recorded for several materials cooled to room temperature and annealed at 600 °C for 50 h are similar to those already reported.[16] Accordingly, the formal valence of bismuth and uranium ions in these oxides has been assumed to be Bi^{3+} and U^{6+}, and the oxygen stoichiometry has been calculated for the electroneutrality of materials. Samples synthesized in this system can be described according to the general formula $Bi_{2-2x}U_xLa_xO_{(3+3x/2)}$, 0.333 ≥ x ≥ 0.038. They can be regarded as superstoichiometric Bi_2O_3 or can be also described in terms of a substoichiometric (MO_2) fluorite of general formula $Bi_{1-x}U_{x/2}La_{x/2}O_{1.5+1.5x/2}$, Z = 4.

Annealed Materials. It is well-known that stabilized fcc-like conductive materials transform gradually on annealing into more ordered low-temperature phases.[19−23] This "aging" phenomenon related to ordering processes occur to a greater or lesser degree in all systems and leads to a lowering of conductivity properties. In general, it limits the technological application of this type of materials; therefore, it is very important to know their structural evolution on annealing. To check the long-term stability of $Bi_{2-2x}U_xLa_xO_{(3+3x/2)}$ oxides, they were subjected to either short (50 h) or long (500 h) annealing periods at 600 °C.

Some hexagonal samples (**C4**, **S4**, **S5**, and **S10** in the compositional range 0.333 ≥ x ≥ 0.167) and the room-temperature stable fcc-type materials (**S11**, **S13** and **C20** (0.154 ≥ x ≥ 0.091)) were annealed at 600 °C for 50 h. In both cases, the annealing process yields hexagonal-type materials, either as a single phase or mixed with monoclinic bismuth oxide. Annealing of the hexagonal samples provokes a larger splitting of diffraction maxima, which becomes more evident as dopant concentration diminishes. The $(c/a)_h$ values (Table 3) deviates significantly from the value $(c/a)_h$ = 2.45 for a face-centered cubic lattice. Cubic **S11** phase (x = 0.154) transforms to hexagonal phase (Figure 3), while for compositions x = 0.133 (**S13**) and x = 0.091 (**C20**) mixtures of hexagonal bismuth uranium lanthanum oxide and α-Bi_2O_3 are formed. The experimental unit cell parameters of the hexagonal phases formed after annealing at 600 °C for 50 h are summarized in Table 3. It is evident that transformation of cubic materials occurs on annealing. Disordered cubic fcc-type oxides

(19) Bevan, D. J. M.; Summerville, E. *Handbook on the Physics and Chemistry of the Rare Earth*; Gschneider, K. A., Jr., Eyring, L., Eds.; North-Holland: Amsterdam, 1989; Vol. 3, p 437.
(20) Allpress, J. G.; Rossell, H. J. *J. Solid State Chem*. **1975**, *15*, 68.
(21) van Dijk, M. P.; Mijlhoff, F. C.; Burggraaf, J. *J. Solid State Chem*. **1986**, *62*, 377.
(22) Whithers, R. L.; Thomson, J. G.; Barlow, P. J. *J. Solid State Chem*. **1991**, *94*, 89.
(23) Watanabe, A.; Drache, M.; Wignacourt, J. P.; Conflant, P.; Boivin, J. C. *Solid State Ionics* **1993**, *67*, 25.

Table 3. Hexagonal Cell Parameters of Samples Annealed to 600 °C for 50 h (S and C Have the Same Meaning as before)

	composition		cell parameters (Å)		
sample	Bi:U:La	x^a	a_h	c_h	c_h/a_h
S4	4:1:1	0.333	3.9937(8)	9.728(2)	2.430
C4	4:1:1	0.333	4.0273(4)	9.546(1)	2.370
S5	5:1:1	0.286	4.018(3)	9.594(7)	2.387
S10	10:1:1	0.167	4.0044(9)	9.536(2)	2.381
S11	11:1:1	0.154	4.0015(3)	9.5429(8)	2.384
S13	13:1:1	0.133	4.0009(7)	9.547(2)	2.380
C20	20:1:1	0.091	3.997(9)	9.61(4)	2.40

[a] Mol % dopant = 100*x*.

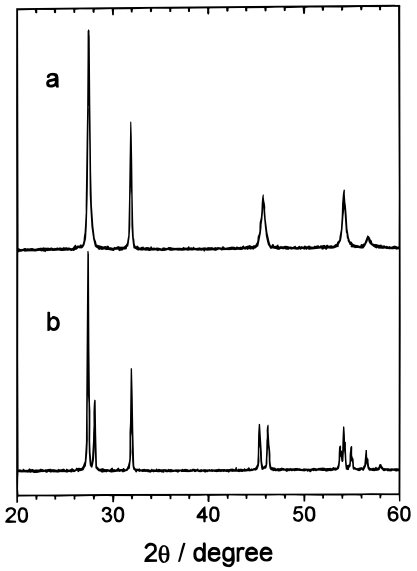

Figure 3. X-ray diffraction patterns recorded for sample $x = 0.154$ (**S11**): (a) as obtained by method I; (b) annealed at 600 °C for 50 h.

transform into more ordered phases with symmetry lower than cubic. On the contrary, hexagonal materials seems to be less affected. However, it can be a misleading result; if the formation of the more ordered phases proceeds through a diffusion mechanism, samples have to be annealed for sufficient time for the diffusion-controlled reaction takes place. Having this in mind, samples synthesized by *methods I* and *II* were annealed at 600 °C for 500 h, and the more significant results are shown below.

According to their behavior, oxides $Bi_{2-2x}U_xLa_xO_{(3+3x/2)}$ can be gathered in the following groups:

(i) $x = 0.333$. The oxide with this composition does not transforms on annealing[16] (Figure 4a).

(ii) $0.286 \geq x \geq 0.25$. X-ray patterns of samples within this compositional range (Figure 4b) show diffraction maxima of the original hexagonal phase, this is particularly evidenced by the presence of the sharp peak at 31.8° (2θ). Some poorly defined maxima are also present. They have been assigned to a new phase that has been isolated as the only phase for the composition $x = 0.222$.

(iii) $x = 0.222$. A new compound with Bi:U:La = 7:1:1 is formed after annealing at 600 °C for 500 h; it is a single phase having the defined composition $Bi_{1.56}U_{0.22}La_{0.22}O_{3.33}$. The X-ray powder pattern is similar to that shown by tetragonal β-Bi_2O_3,[17] and in a first approximation it has been indexed on the basis of a tetragonal cell with parameters $a_t = 7.806$ and $c_t = 5.768$ Å (Figure 4c).

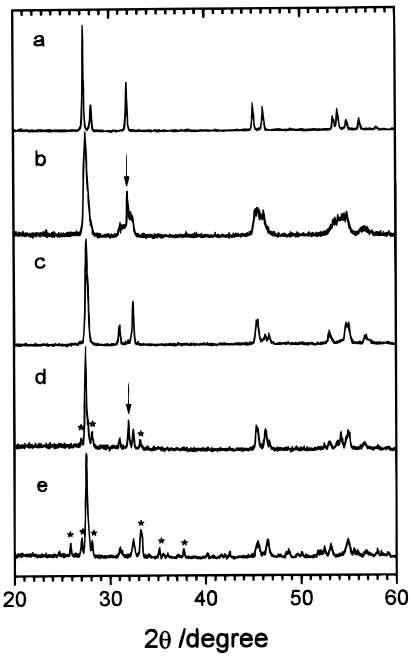

Figure 4. X-ray diffraction patterns of $Bi_{2-2x}U_xLa_xO_{(3+3x/2)}$ annealed at 600 °C for 500 h; (a) $x = 0.333$; (b) $x = 0.25$; (c) $x = 0.222$; (d) $x = 0.167$; (e) $x = 0.091$. *α-Bi_2O_3; only maxima below 40° (2θ) are marked. Arrowed peak corresponds to the reflection (012) ≈ 27.5° (2θ) of the hexagonal phase.

(iv) $0.167 \geq x \geq 0.133$. A mixture of the new "tetragonal" phase, monoclinic Bi_2O_3 and the original hexagonal phase is identified (Figure 4d).

(v) $0.118 \geq x \geq 0.091$. A mixture of the "tetragonal" phase and α-Bi_2O_3 is formed (Figure 4e).

These results can be summarized as follows: only the oxide $Bi_{1.34}U_{0.33}La_{0.33}O_{3.48}$ does not alter on annealing; oxides $Bi_{2-2x}U_xLa_xO_{(3+3x/2)}$ ($0.286 \geq x \geq 0.091$) transform into the so-called "tetragonal" phase, either as a single phase ($x = 0.222$) or mixed with the original hexagonal phase, with α-Bi_2O_3, or with both. This result clearly show the remarkable tendency of these materials to transform into more-ordered phases.

Thermal Stability. The evolution of materials when they are subjected to dynamic heating processes have been determined by thermal analysis. Thermogravimetric curves show only a plateau within the temperature range explored (room temperature to 950 °C), indicating that the samples do not undergo significant weight change along the dynamical heating treatments. DTA curves recorded to 950 °C for quenched fcc-like phases show patterns identical with those already reported for the oxide with $x = 0.333$.[16] DTA curves of hexagonal materials in the compositional range $0.333 \geq x \geq 0.250$ show a very weak endothermic effect in the temperature range 800−880 °C ascribed to the reversible hexagonal ⇄ cubic transition. This peak is not observed in thermograms recorded for hexagonal materials with composition $x = 0.222$ (**C7**) (Figure 5a1) and 0.200 (**C8**), even though residues have the fluorite-type structure. This result shows that from a certain amount of dopant, the phase transition is very sluggish and takes place progressively in a wide range of temperature. Finally, DTA curves of the stabilized cubic phases with compositions $x \leq 0.154$ do not show any thermal effect up to 950 °C.

The DTA curve of "tetragonal" $Bi_{1.56}U_{0.22}La_{0.22}O_{3.33}$ single phase recorded to 950 °C at 10 °C min^{-1} heating

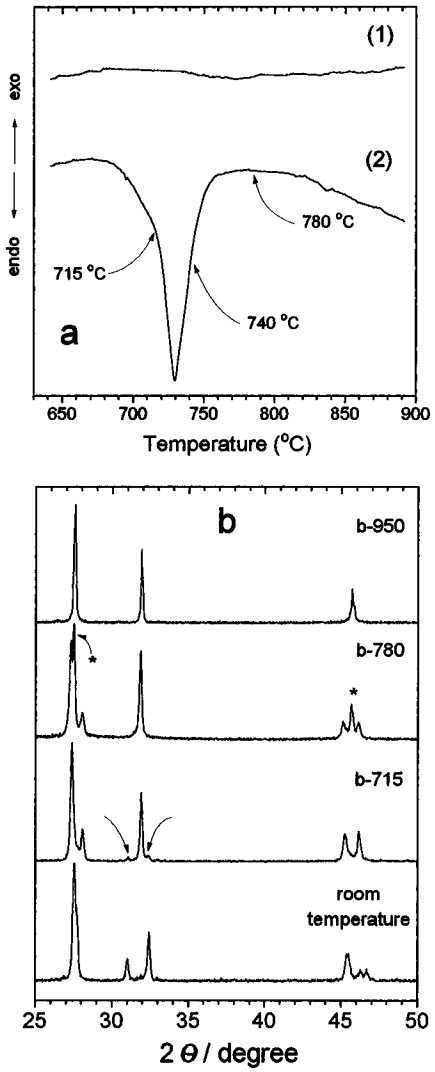

Figure 5. (a) DTA curves of sample $x = 0.222$ (**C7**): (1) original hexagonal phase; (2) "tetragonal" phase formed after annealing at 600 °C for 500 h; (b) X-ray diagrams of the "tetragonal" phase quenched from the temperatures indicated in each pattern.

rate, is presented in Figure 5a2. It only shows an asymmetric endothermal effect between 680 and 760 °C (T_{max} = 730 °C). The X-ray diagram of the residue (Figure 5b-950) corresponds to a fluorite-type material. To establish the pathway of the "tetragonal" → cubic transformation, batches of the original "tetragonal" phase were kept at some definite temperatures for 1 h in the DTA equipment and then quenched to room temperature by rapidly removing the furnace. Temperatures are arrowed in the thermogram (Figure 5a2) and X-ray patterns recorded for quenched samples are shown in Figure 5b. After 1 h at 715 °C a mixture of hexagonal (major phase) and "tetragonal" phases is identified (Figure 5b-715). After 1 h at 740 °C, the residue corresponds to a mixture of hexagonal and fcc-type phases, this latter being the minor component in the mixture. The diagram of the "tetragonal" sample quenched from 780 °C (1 h) shows that the cubic phase has considerably increased but the amount of hexagonal phase is still important (Figure 5b-780). Nevertheless, to complete the hexagonal → cubic transformation, the sample must be heated above this latter temperature (Figure 5b-950). The reversibility of the latter cubic → hexagonal transformation was checked by cooling the sample from 950 °C at 10 °C min^{-1}. The X-ray diagrams are identical with that displayed in Figure 2a and identical with that recorded for the original hexagonal material with identical composition (**C7**). This proves that we are dealing with a reversible phase transition.

From these results it can be pointed out that in the first stage of the reaction (690−715 °C) "tetragonal" phase irreversibly transforms into the hexagonal phase. Later on, the reversible hexagonal ⇄ cubic transformation takes place and causes the appearance of the endothermic effect at 715−760 °C. As has been indicated above, it is worth noting that the DTA curve of the original nonannealed hexagonal phase (sample **C7**) does not show any endotherm caused by the hexagonal ⇄ cubic phase transition (Figure 5a1). However, in the annealed material, this transition takes place in a narrow temperature interval (Figure 5a2). It suggests that **only** the just-formed hexagonal phase arising from the "tetragonal" → hexagonal transition rapidly transforms into the fluorite-type phase. This hypothesis was confirmed by the following experiment: batches of the "tetragonal" material quenched from 740 °C (mixture of hexagonal and cubic phases) were kept to 760 and 780 °C for 1 h and then quenched to room temperature. The X-ray patterns of the quenched samples show that the hexagonal ⇄ cubic phase transition does not proceed further and the hexagonal/cubic ratio remains almost constant.

Discussion and Conclusions

Figure 6 summarizes phases identified in the $Bi_{2-2x}U_xLa_xO_{(3+3x/2)}$ system in the compositional range $0.333 \geq x \geq 0.038$. It is worth mentioning the formation of a cubic phase in the $Bi-U^{6+}-O$ system for compositions ranging between Bi:U = 4:1 and 14:1 and cell parameters from 5.645 to 5.595 Å has been reported.[24] Studies carried out in the system $Bi_2O_3-Ln_2O_3$ (Ln = La−Yb) show that lanthanum-doped bismuth oxide with the cubic fluorite-type structure has never been obtained, even for quenched specimens.[25] This work shows that when bismuth oxide is simulataneously doped with uranium and lanthanum in U:La = 1:1 ratio, stabilization of the fluorite-type phase at room temperature can be attained.

Method I yields the fcc-type phase as a single phase at room temperature, in the compositional range $Bi_{2-2x}U_xLa_xO_{(3+3x/2)}$ ($0.154 \geq x \geq 0.133$). For higher dopant content ($0.333 \geq x \geq 0.167$), quenching of the samples from the synthesis temperature (950 °C) leads to the formation of the fluorite-type materials. Figure 7 shows the variation with composition of the cubic cell lattice for stabilized and quenched fcc-type oxides. The cell dimension linearly diminishes as the dopant content decreases. It goes from 5.6378(1) for $x = 0.25$ (**S4**) to 5.6038(2) Å for $x = 0.118$ (**S15**). From the latter composition and to the limit explored ($x = 0.038$, **S50**), mixtures of a cubic phase and increasing amounts of α-Bi_2O_3 are identified at room temperature. The lattice parameter of the cubic phase remains almost constant and close to the **S15** sample. This result suggest $x \approx 0.118$ as the lower limiting composition at room tem-

(24) Rüdorf, W.; Erfurth, H. *Z. Naturforsch.* **1966**, *21B*, 85.
(25) Iwahara, H.; Esaka, T.; Sato, T.; Takahashi, T. *J. Solid State Chem.* **1981**, *39*, 173.

Method I: quenched from 950 °C	■	■	■			■	■								
Method I cooled within the furnace	⊙	⊙	⊙			⊙	⊙	■		■	■ △	■ △	■ △		■ △
Method II	⊙	⊙	⊙	⊙	⊙		⊙ ■		■ ⊙		■		■	■	
Annealed to 600 °C for 50h	⊙	⊙					⊙	⊙		⊙				⊙ △	
Annealed to 600 °C for 500h	⊙	⊙ ⊠	⊠ ⊙	⊠	⊠ ⊙ △		⊠ ⊙	⊠ ⊙ △		⊠ ⊙ △	⊠ △		⊠ △	⊠ △	
x in $Bi_{2-2x}U_xLa_xO_{3+3x/2}$	.333	.286	.25	.222	.20	.182	.167	.154	.138	.133	.118	.111	.105	.091	.038
N in Bi:U:La = N:1:1	4	5	6	7	8	9	10	11	12.5	13	15	16	17	20	50

■ = fluorite-type structure; ⊙ = hexagonal; ⊠ = "tetragonal"; △ = α-Bi_2O_3

Figure 6. Summary of phases identified in the $Bi_{2-2x}U_xLa_xO_{(3+3x/2)}$ system, in the compositional range $0.333 \geq x \geq 0.038$.

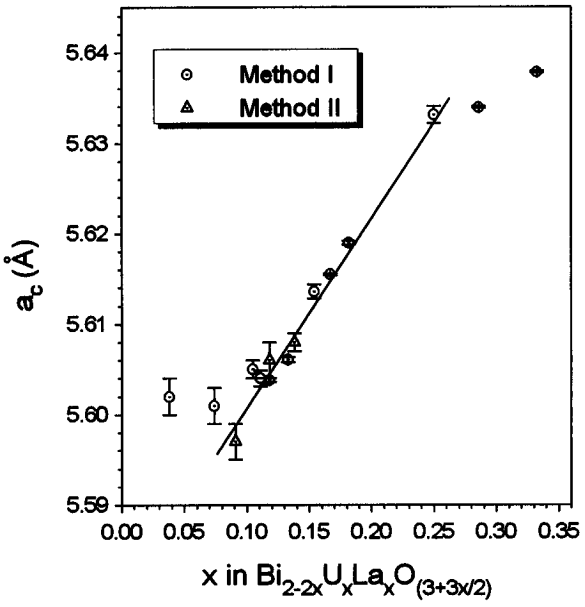

Figure 7. Cubic cell parameter a_c (Å) vs composition, for the fcc-type phases synthesized by *methods I* and *II*.

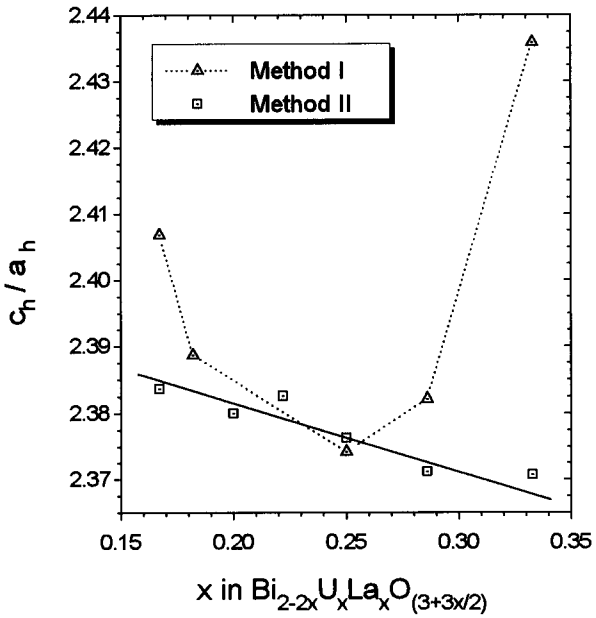

Figure 8. c_h/a_h vs composition for hexagonal phases synthesized by *methods I* and *II*.

perature for the fluorite-type phase synthesized by *method I*. For the highest dopant concentrations $x > 0.25$, a deviation from the linearity is observed. *Method II* allows the stabilization at room temperature of the cubic material as an only phase in a compositional range ($0.118 \geq x \geq 0.091$), which is slightly wider than for *method I*. In this case, the cell parameter linearly decreases to 5.597(2) Å for $x = 0.091$ (**C20**) (see Table 2 and Figure 7). This result can be accounted on the basis of the low heating/cooling rates used and, consequently, the more extended reaction time. Therefore, diffusion of minor dopant cations within the Bi_2O_3 matrix is favored.

For analogous dopant concentration, cubic cell parameter (Table 2) has values similar to those reported for the fcc samples in the $Bi-U^{6+}-O$[24], $Bi_2O_3-Ln_2O_3$ (Ln = Y,[26] Gd[27]) and $Bi_2O_3-WO_3$[12] systems. In general, a_c decreases on increasing the dopant content; however, in our case just the opposite variation occurs, showing the same trend observed for the fcc-type oxides formed in the $Bi-U^{6+}-O$[24] system. To account for this effect, several contributions could be considered: (i) the introduction of some extra oxygen atoms into the nonoccupied oxygen positions in the δ-Bi_2O_3 structure to balance the highly charged U^{6+} dopant cation; (ii) the high ionic radii of the La^{3+} cations.

On the other hand, when the dopant concentration is high (hexagonal region), samples synthesized by *method II* show a small variation of the c_h/a_h ratio (Figure 8), ranging from 2.37 ($x = 0.333$, **C4**) to 2.38 ($x = 0.167$, **C10**), while materials with the same composition prepared by *method I* show that the c_h/a_h ratio strongly depend upon composition, with values generally higher than those determined for materials synthesized by *method II* (Table 1). Moreover, all the hexagonal

(26) Takahashi, T.; Iwahara, H.; Arao, T. *J. Appl. Electrochem.* **1975**, *5*, 187.

(27) Takahashi, T.; Esaka, T.; Iwahara, H. *J. Appl. Electrochem.* **1975**, *5*, 197.

samples show a cell parameter c_h smaller than that calculated from the geometrical relationship $c_h = a_c\sqrt{3}$, indicating that the experimental hexagonal cell is squatted along the *c* axis. This effect is independent of the dopant content.

It is also worth to emphasize that aging of materials yields the "tetragonal" phase which is formed as the only phase for $x = 0.222$. It is plausible to assume that the annealing to 600 °C provokes the diffusion of cations, leading to the formation of a more-ordered phase. On this basis, the evolution cubic → hexagonal → "tetragonal" experienced by the materials on annealing can be accounted for. Having this in mind, the differences existing between samples with identical composition but synthesized by either *method I* or *II* can be justified. For example, the material with $x = 0.333$ synthesized by *method II* (**C4**) shows a c_h/a_h ratio that deviates from the particular value $c_h/a_h = 2.45$, more than **S4**, synthesized by *method I* (Table 1). The very low cooling rate used in the former case (2 °C h^{-1} from 800 to 600 °C and 1 °C min^{-1} from 600 °C to room temperature) would favor the diffusion of cations, which get to a more ordered distribution. As the arrangement of the cations in the layers stacked along the $[111]_c$ departs from the random distribution assumed for the fluorite-type structure, they shift more away from their equilibrium positions in the fcc-type structure, yielding hexagonal fluorite-related materials, as it has been already shown by electron diffraction studies.[16] Finally, it can also be pointed out that fcc-type phases are all metastable; they are more or less easily stabilized to room temperature depending upon dopant concentration. When they are treated over a short period (50 h) to 600 °C, they all transform to hexagonal. Moreover, except $Bi_{1.34}U_{0.33}La_{0.33}O_{0.33}$, hexagonal phases are also metastable. When they are treated over a long period (500 h) to 600 °C, they gradually transform to the "tetragonal" phase, which constitutes the more ordered arrangement of cations in the system. It is worth indicating that the "tetragonal" phase is associated to cations ordering and different from that associated with oxygen vacancy ordering reported for $(Bi_2O_3)_{0.80}(Er_2O_3)_{0.20}$ and $(Bi_2O_3)_{0.75}(Y_2O_3)_{0.25}$.[28]

It must also be stressed that materials aged to 600 °C for 500 h, even if they consist of a mixture of phases (Figure 6), can be regenerated when they are subjected to the original synthesis conditions. Finally, conductivity measurements carried out for some compositions[16] show that these compounds can be included in the group of the best bismuth-based oxygen-ion conductors.

Acknowledgment. The authors thank Mr. J. Bueno for technical assistance with thermal analysis. This work has been supported by CICyT Project MAT 92/0202.

CM950345U

(28) Jinag, N.; Buchanam, R. M.; Henn, F. E. G.; Marshall, A. F.; Stevenson, D. A. *Mater. Res. Bull.* **1994**, *29*, 247.